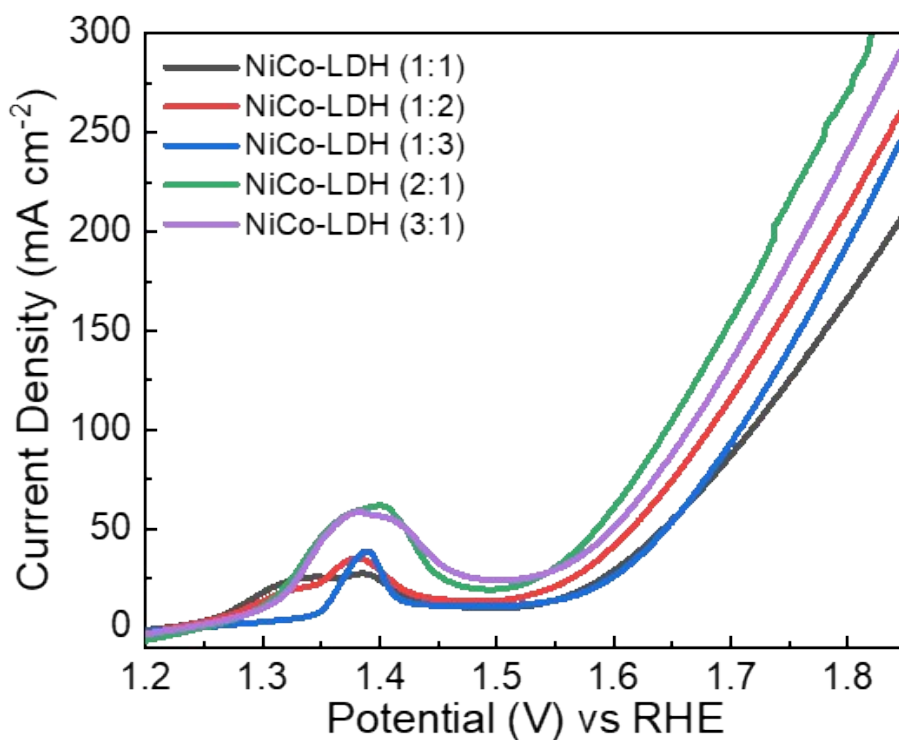


## Supporting Information

### Bifunctional catalytic activity of a Ni-Co layered double hydroxide for the electro-oxidation of water and methanol

*Komal Patil<sup>a</sup>, Pravin Babar<sup>a</sup>, Dong Min Lee<sup>a</sup>, Vijay Karade<sup>a</sup>, Eunae Jo<sup>a</sup>, Sumit Korade<sup>ab</sup>, and  
Jin Hyeok Kim<sup>a\*</sup>*



**Figure S1** OER polarization curves of NiCo-LDH with different molar ratio

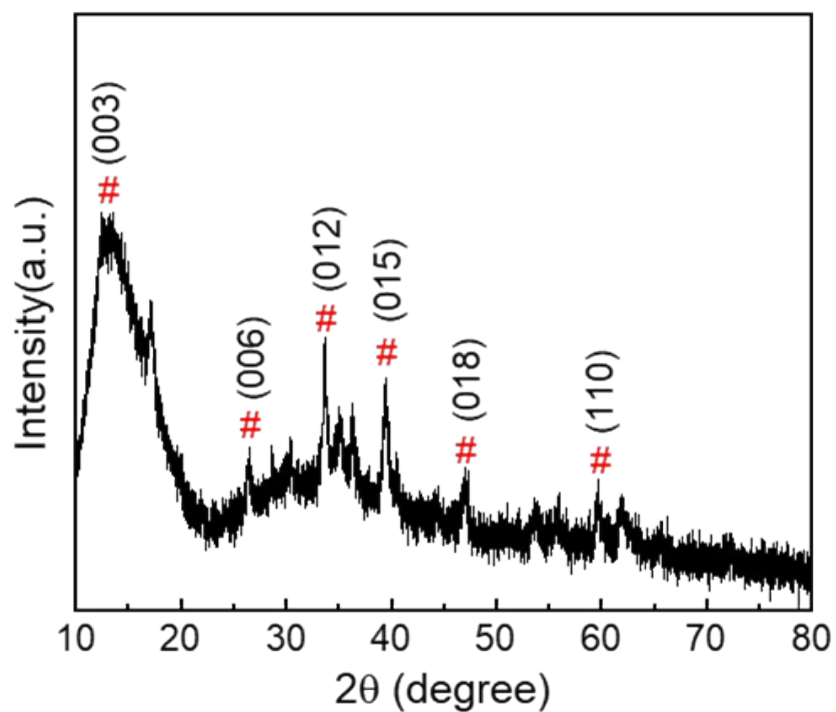


**Figure S2** XRD spectra of the powder sample of NiCo-LDH

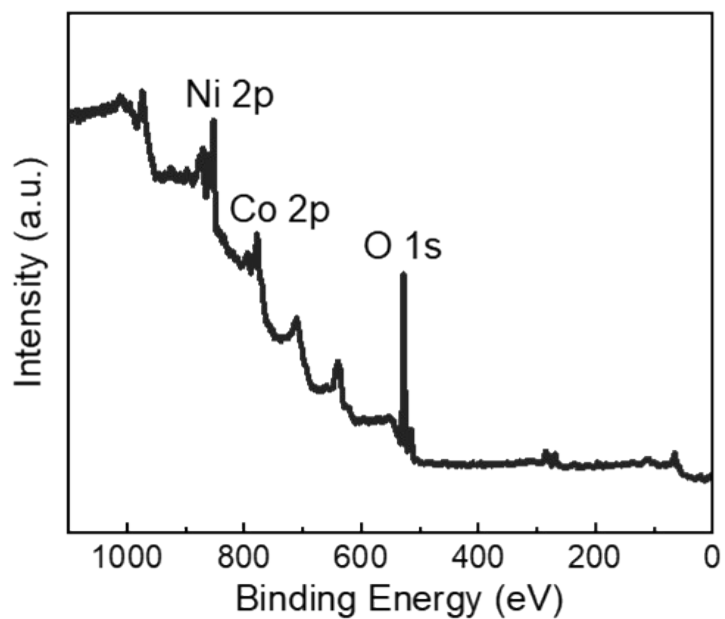


**Figure S3** High-resolution XPS survey spectrum of NiCo-LDH nanowires

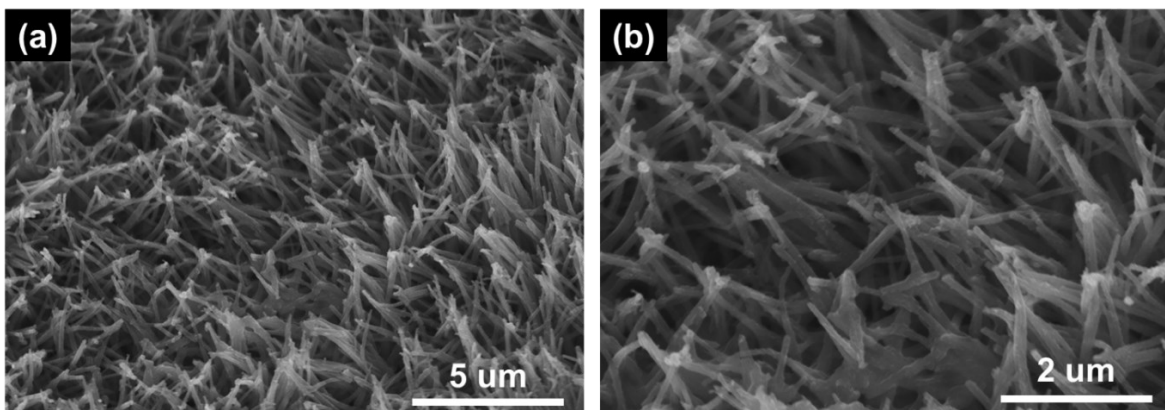


**Figure S4** FE-SEM images of NiCo-LDH nanowires after 50 h stability

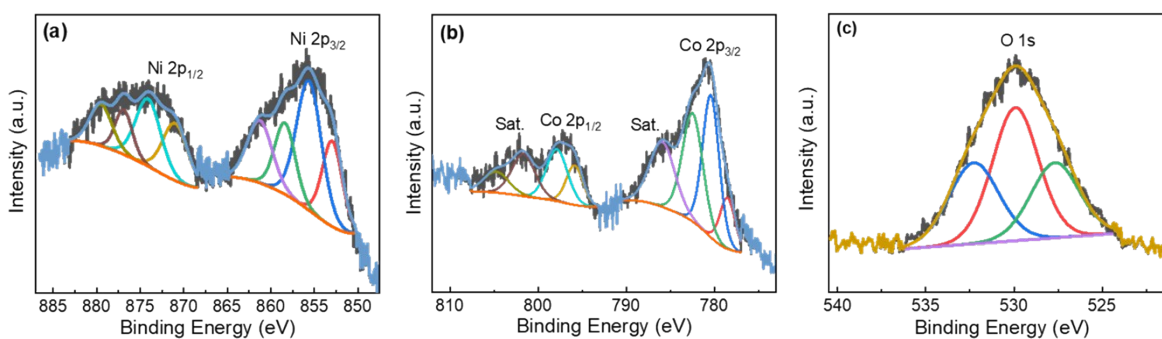


**Figure S5** XPS spectra of NiCo-LDH nanowires (a) spectrum of Ni 2p (b) spectrum of Co 2p (c) spectrum of O 1s after 50 h stability in 1 M KOH

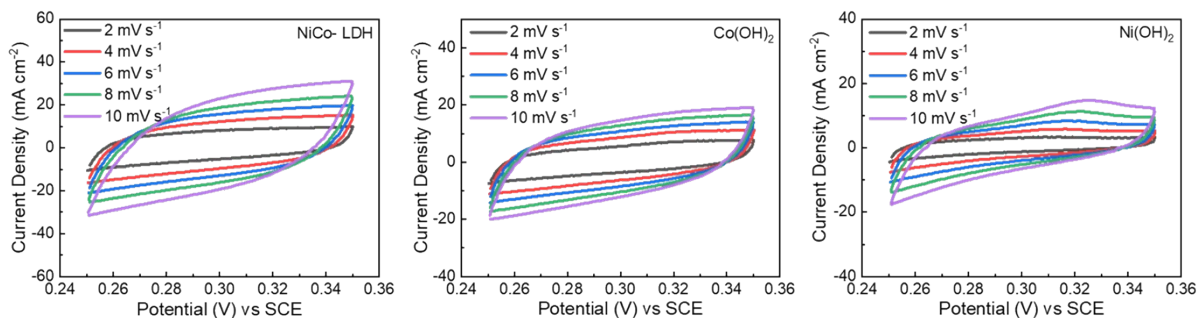


**Figure S6** CV curves of NiCo-LDH,  $\text{Co(OH)}_2$ , and  $\text{Ni(OH)}_2$  in 1 M KOH at different scan rates

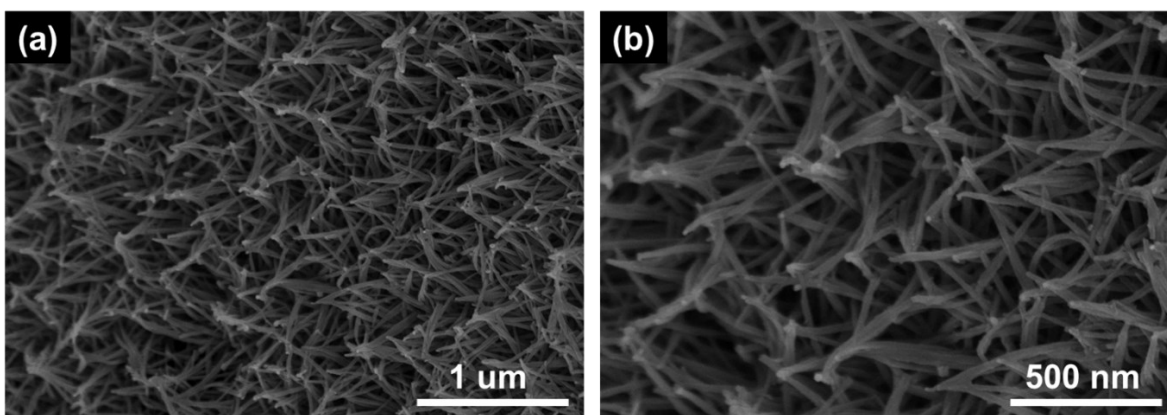


**Figure S7** FE-SEM images of NiCo-LDH nanowires after 2000 s stability for MOR in 1M KOH with 0.5 M methanol

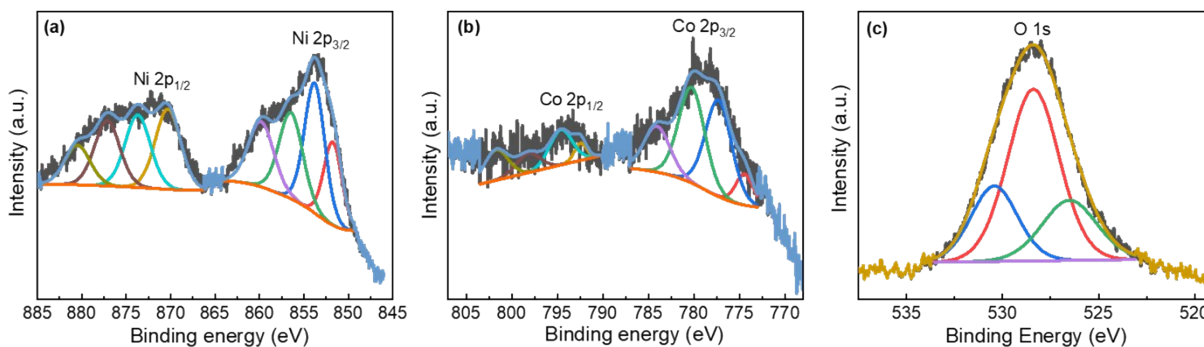


**Figure S8** XPS spectra of NiCo-LDH nanowires (a) spectrum of Ni 2p (b) spectrum of Co 2p (c) spectrum of O 1s after 2000 s stability in 1 M KOH with 0.5 M methanol

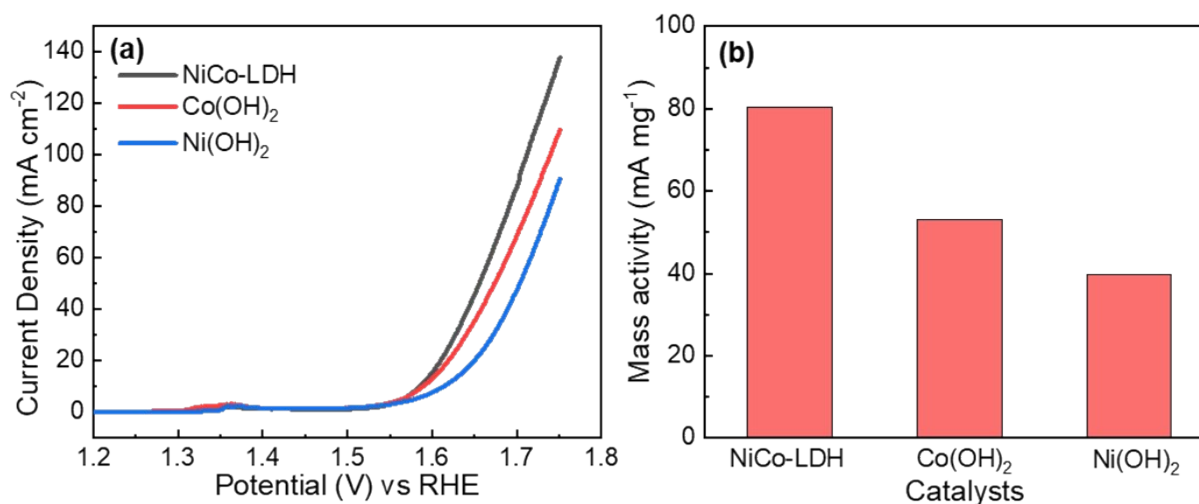


**Figure S9** (a) OER polarization curves of NiCo-LDH, Co(OH)<sub>2</sub>, and Ni(OH)<sub>2</sub> deposited on glassy carbon electrode. (b) Corresponding mass activities of NiCo-LDH, Co(OH)<sub>2</sub>, and Ni(OH)<sub>2</sub> deposited on glassy carbon electrode at potential of 1.7 V.

#### **Preparation of NiCo-LDH, Co(OH)<sub>2</sub>, and Ni(OH)<sub>2</sub> on glassy carbon electrode**

The NiCo-LDH or Co(OH)<sub>2</sub> or Ni(OH)<sub>2</sub> also deposited onto a glassy carbon electrode (GC). To prepare NiCo-LDH on the GC electrode, 5 mg of NiCo-LDH was dispersed in 1 mL of a mixed solution containing 495  $\mu$ L of ethanol, 490  $\mu$ L of water, and 15  $\mu$ L of 5 Wt.% Nafion solution. The mixture was then sonicated to form a homogeneous catalyst ink. Then the catalyst ink was drop casted on the surface of the 0.07 cm<sup>2</sup> GC electrode and dried in air. The amount of NiCo-LDH loaded onto the GC electrode was approximately 1.1 mg cm<sup>-2</sup>. The same procedure was applied to deposit Ni(OH)<sub>2</sub> and Co(OH)<sub>2</sub>.

**Figure S9 (a)** shows the OER polarization curve obtained with NiCo-LDH, Co(OH)<sub>2</sub>, and Ni(OH)<sub>2</sub> deposited onto the GC electrode. The mass activity values of NiCo-LDH, Co(OH)<sub>2</sub>, and Ni(OH)<sub>2</sub> are 80.34, 53.04, and 39.80 mA mg<sup>-1</sup> respectively (**Figure S9 (b)**).

**Table S1** Comparison of OER performances with previously reported NiCo-based electrocatalysts

Catalyst	$\eta$ (mV) at $10 \text{ mA} \cdot \text{cm}^{-2}$	Tafel slope ( $\text{mV} \cdot \text{dec}^{-1}$ )	Electrolyte	ref
Ni-Co Nanowire	302	43.6	1 M KOH	S1
NiCo-LDH nanoarrays	307	64	1 M KOH	S2
NiCo-LDH nanosheets arrays	271	72	1 M KOH	S3
$\text{Ni}_x\text{Co}_{2x}(\text{OH})_{6x}@$ graphene	280	67	1 M KOH	S4
NiOOH–NiCr <sub>2</sub> O <sub>4</sub> nanosheets	271 ( $20 \text{ mA} \cdot \text{cm}^{-2}$ )	104	1 M KOH	S5
NiO/NiCo <sub>2</sub> O <sub>4</sub> Nanocrystals	264	79.4	1 M KOH	S6
NiCo/NiCoO <sub>x</sub> -FeOOH	278	47.5	1 M KOH	S7
NiCoFe-LDH	280	34	1 M KOH	S8
$\text{Ni}_x\text{Co}_{1-x}(\text{OH})_2$ nanoplate	270	59	1 M KOH	S9
U-NiO/NiCo <sub>2</sub> O <sub>4</sub>	387	49	0.1 M KOH	S10
C-NiO/NiCo <sub>2</sub> O <sub>4</sub>	430	44	0.1 M KOH	S10
NiO/NiCo <sub>2</sub> O <sub>4</sub> nanosheets	360	61	1 M NaOH	S11
NiCo <sub>2</sub> O <sub>4</sub>	430	139	1 M NaOH	S11
NiO/NiCo <sub>2</sub> O <sub>4</sub> nanocrystals	264	79.3	1 M KOH	S12
NiCo <sub>2</sub> O <sub>4</sub> on stainless steel	530	49	0.1 M NaOH	S13
NiCo <sub>2</sub> O <sub>4</sub> nanoframes (Cu <sub>2</sub> O)	265	82	1 M KOH	S14
NiCo <sub>2</sub> O <sub>4</sub> nanowires	460	90	1 M KOH	S15
MOF-NiO/ NiCo <sub>2</sub> O <sub>4</sub>	410	49	0.1 M KOH	S16
NiCo-LDH	270 ( $20 \text{ mA cm}^{-2}$ )	82	1 M KOH	This work

**Table S2** Comparison of current densities, scan rate and applied potential with previously reported NiCo-based electrocatalyst for MOR in 1 M KOH

Electrocatalyst	Methanol Concentration/mol L <sup>-1</sup>	Scan Rate/mV s <sup>-1</sup>	Applied Voltage	Current Density/mA cm <sup>-2</sup>	Ref
NiCo <sub>2</sub> O <sub>4</sub> nanosheet	0.5	10	0.6 V vs. SCE	111	17
NiO nanosheet @ nanowire	0.5	10	1.62 V vs. RHE	89	18
NiCo <sub>2</sub> O <sub>4</sub> nanocloth	0.5	10	0.6 V vs. SCE	134	17
NiO nanosheets	0.5	50	0.7 V vs. Ag/AgCl	85.3	19
NiCo <sub>2</sub> O <sub>4</sub> /carbon xerogel	0.5	50	0.6 V vs. Ag/AgCl	98	20
Ni/Graphene	0.75	50	0.728 V vs. Ag/AgCl	147.108	21
NiMoO <sub>4</sub> /C	2.0	50	0.8 V vs Hg/HgO	49	22
Mesoporous NiCo <sub>2</sub> O <sub>4</sub>	0.5	10	0.6 V vs.Hg/HgO	125	23
Co <sub>3</sub> O <sub>4</sub> / NiCo <sub>2</sub> O <sub>4</sub>	0.5	10	0.6 V vs. Hg/HgO	140	24
NiCo-LDH	0.5	10	0.5 V vs. SCE	761	This work

## References

- S1) L. Xu, Q.Q. Jiang, Z.H. Xiao, X.Y. Li, J. Huo, S.Y. Wang, L.M. Dai, Plasma-Engraved Co<sub>3</sub>O<sub>4</sub> Nanosheets with Oxygen Vacancies and High Surface Area for the Oxygen Evolution Reaction, *Angew. Chem. Int. Ed.* 55 (2016) 5277-5281.
- S2) C. Yu, Z.B. Liu, X.T. Han, H.W. Huang, C.T. Zhao, J. Yang, J.S. Qiu, NiCo-layered double hydroxides vertically assembled on carbon fiber papers as binder-free high-active electrocatalysts for water oxidation, *Carbon* 110 (2016) 1-7.
- S3) W.J. Liu, J. Bao, M.L. Guan, Y. Zhao, J.B. Lian, J.X. Qiu, L. Xu, Y.P. Huang, J. Qian, H.M. Li, Nickel–cobalt-layered double hydroxide nanosheet arrays on Ni foam as a bifunctional electrocatalyst for overall water splitting, *Dalton Trans.* 46 (2017) 8372-8376.

- S4) J.H. Shi, N.X. Du, W.J. Zheng, X.C. Li, Y. Dai, G.H. He, Ultrathin Ni-Co double hydroxide nanosheets with conformal graphene coating for highly active oxygen evolution reaction and lithium ion battery anode materials, *Chem. Eng. J.* 327 (2017) 9–17.
- S5) J.X. Zhao, X. Ren, Q.Z. Han, D.W. Fan, X. Sun, X. Kuang, Q. Wei, D. Wu, Ultra-thin wrinkled NiOOH–NiCr<sub>2</sub>O<sub>4</sub> nanosheets on Ni foam: an advanced catalytic electrode for oxygen evolution reaction, *Chem. Commun.* 54 (2018) 4987–4990.
- S6) C. Chang, L. Zhang, C.-W. Hsu, X.-F. Chuah, S.-Y. Lu, Mixed NiO/NiCo<sub>2</sub>O<sub>4</sub> Nanocrystals Grown from the Skeleton of a 3D Porous Nickel Network as Efficient Electrocatalysts for Oxygen Evolution Reactions, *ACS Appl. Mater. Interfaces* 10 (2018) 417–426.
- S7) Y.B. Shao, M.Y. Zheng, M.M. Cai, L. He, C.L. Xu, Improved Electrocatalytic Performance of Core-shell NiCo/NiCoO<sub>x</sub> with amorphous FeOOH for Oxygen-evolution Reaction, *Electrochim. Acta* 257 (2017) 1–8.
- S8) T. Wang, W. C. Xu, H. X. Wang, Ternary NiCoFe Layered Double Hydroxide Nanosheets Synthesized by Cation Exchange Reaction for Oxygen Evolution Reaction, *Electrochim. Acta* 257 (2017) 118–127.
- S9) Q. Ye, J. Li, X. Liu, X. Xu, F. Wang, B. Li, Surface pattern of Ni-Co hydroxide nanoplate arrays electrocatalysts for the oxygen evolution reaction, *J. Power Sources* 412 (2019) 10-17.
- S10) A. Cetin, E.N. Esenturk, Hierarchical nanowire and nanoplate-assembled NiCo<sub>2</sub>O<sub>4</sub>-NiO biphasic microspheres as effective electrocatalysts for oxygen evolution reaction, *j.mtchem*, 14 (2019) 100215.
- S11) C. Mahala, M. Basu, Nanosheets of NiCo<sub>2</sub>O<sub>4</sub>/NiO as efficient and stable electrocatalyst for oxygen evolution reaction, *ACS Omega* 2 (2017) 7559e7567, <https://doi.org/10.1021/acsomega.7b00957>.
- S12) C. Chang, L. Zhang, C.-W. Hsu, X.-F. Chuah, S.-Y. Lu, Mixed NiO/NiCo<sub>2</sub>O<sub>4</sub> nanocrystals grown from the skeleton of a 3D porous nickel network as efficient electrocatalysts for oxygen evolution reactions, *ACS Appl. Mater. Interfaces* 10 (2018) 417e426, <https://doi.org/10.1021/acsomega.7b13127>.
- S13) I. Barauskienė, E. Valatka, Layered nickel-cobalt oxide coatings on stainless steel as an electrocatalyst for oxygen evolution reaction, *Electrocatalysis* 10 (2019) 63e71, <https://doi.org/10.1007/s12678-018-0495-x>.
- S14) Z. Chen, B. Zhao, Y.-C. He, H.-R. Wen, X.-Z. Fu, R. Sun, C.-P. Wong, NiCo<sub>2</sub>O<sub>4</sub> nanoframes with a nanosheet surface as efficient electrocatalysts for the oxygen evolution reaction, *Mater. Chem. Front.* 2 (2018) 1155e1164, <https://doi.org/10.1039/C8QM00027A>.



S15) X. Yu, Z. Sun, Z. Yan, B. Xiang, X. Liu, P. Du, Direct growth of porous crystalline NiCo<sub>2</sub>O<sub>4</sub> nanowire arrays on a conductive electrode for high-performance electrocatalytic water oxidation, *J. Mater. Chem. A* 2 (2014) 20823e20831, <https://doi.org/10.1039/C4TA05315J>.

S16) Y. Wang, Z. Zhang, X. Liu, F. Ding, P. Zou, X. Wang, Q. Zhao, H. Rao, MOF-derived NiO/NiCo<sub>2</sub>O<sub>4</sub> and NiO/NiCo<sub>2</sub>O<sub>4</sub>-rGO as highly efficient and stable electrocatalysts for oxygen evolution reaction, *ACS Sustain. Chem. Eng.* 6 (2018) 12511e12521, <https://doi.org/10.1021/acssuschemeng.8b03221>.

S17) W. Wang, Q. Chu, Y. Zhang, W. Zhu, X. Wang, X. Liu, Nickel foam supported mesoporous NiCo<sub>2</sub>O<sub>4</sub> arrays with excellent methanol electro-oxidation performance, *New J. Chem.* 39 (2015) 6491–6497.

S18) Q. Luo, M. Peng, X. Sun, A.M. Asiri, Hierarchical nickel oxide nanosheet @ nanowire arrays on nickel foam: an efficient 3D electrode for methanol electro-oxidation, *Catal. Sci. Technol.* 6 (2016) 1157–1161.

S19) W.L. Yang, X.P. Yang, J. Jia, C.M. Hou, H.T. Gao, Y.N. Mao, C. Wang, J.H. Lin, X.L. Luo, Oxygen vacancies confined in ultrathin nickel oxide nanosheets for enhanced electrocatalytic methanol oxidation, *Appl. Catal. B-Environ.* 244 (2019) 1096–1102.

S20) M.M. El-Deeb, W.M.A. El Rouby, A. Abdelwahab, A.A. Farghali, Effect of pore geometry on the electrocatalytic performance of nickel cobaltite/ carbon xerogel nanocomposite for methanol oxidation, *Electrochim. Acta* 259 (2018) 77–85.

S21) N. Ullah, M. Xie, C.J. Oluigbo, Y. Xu, J. Xie, H.U. Rasheed, M. Zhang, Nickel and cobalt in situ grown in 3-dimensional hierarchical porous graphene for effective methanol electro-oxidation reaction, *J. Electroanal. Chem.* 838 (2019) 7–15.

S22) P.R. Jothi, S. Kannan, G. Velayutham, Enhanced methanol electro-oxidation over in-situ carbon and graphene supported one dimensional NiMoO<sub>4</sub> nanorods, *J. Power Sources* 277 (2015) 350–359.

S23) R. Ding, L. Qi, M.J. Jia, H.Y. Wang, Sodium dodecyl sulfate-assisted hydrothermal synthesis of mesoporous nickel cobaltite nanoparticles with enhanced catalytic activity for methanol electrooxidation, *J. Power Sources* 251 (2014) 287–295.

S24) L. Qian, S. Luo, L. Wu, X. Hu, W. Chen, X. Wang, In situ growth of metal organic frameworks derived hierarchical hollow porous Co<sub>3</sub>O<sub>4</sub>/NiCo<sub>2</sub>O<sub>4</sub> nanocomposites on nickel foam as self-supported flexible electrode for methanol electrocatalytic oxidation, *J. Power Sources* 503 (2020) 144306.